Analysis of electric field control methods for foil coils in high-voltage linear actuators

T.A. van Beek, J.W. Jansen, E.A. Lomonova

Eindhoven University of Technology
Electrical Engineering
Groene Loper 19, 5612AZ Eindhoven, the Netherlands
e-mail: t.a.v.beek@tue.nl

Abstract: This paper describes multiple electric field control methods for foil coils in high-voltage coreless linear actuators and their sensitivity to misalignment. The investigated field control methods consist of resistive, refractive, capacitive and geometrical solutions for mitigating electric stress at edges and corners of foil coils. These field control methods are evaluated using 2-D boundary element and finite element methods. A comparison is presented between the field control methods and their ability to mitigate electric stress in coreless linear actuators. Furthermore, the sensitivity to misalignment of the field control methods is investigated.

Key words: electric field control methods, high-voltage, linear actuators, sensitivity analysis, stress grading

1. Introduction

Increasing demands of the throughput of high-precision positioning systems require more powerful actuators in the positioning systems. Therefore, the power dissipation in these systems is increased and larger volumes of heavy power cables are necessary. This results in larger force disturbances which negatively affect the accuracy of the positioning stage. To decrease force disturbances and the cable mass, the operating voltage of the actuators is increased to above 2000 V. As a result, partial discharges occur during the expected lifetime of an inverter-fed actuator [1]. To ensure that the linear actuators reach their expected lifetime, electric field control methods have to be employed as is performed in cable accessories of medium and high-voltage networks [2-5] and high-voltage rotating machines [6-8]. These electric field control methods mitigate electric field stress and, therefore, ensure the partial discharge inception voltage is above the operating voltage. However, the field control methods in rotating machines are not applicable to coreless linear actuators. In rotating machines, field control methods focus mainly on reducing the stress near slot terminations and along the end-turns [9] whereas in coreless

linear actuators with foil coils high electric field strengths occur near the edge of the inner or outer turn of the coils [10].

In this paper, multiple electric field control methods for foil coils in high-voltage linear actuators are analyzed using boundary element and finite element methods. Furthermore, their ability to mitigate electric stress in coreless linear actuators is compared and the sensitivity to misalignment of the placement of field control methods with respect to the coil is investigated.

2. Analysis method

The effect of each field control method on the electric field distribution is evaluated in conjunction with a high-power density coreless linear actuator configuration. A section of this configuration, shown in Figure 1 comprises a water-cooling environment, which is connected to Protective Earth (PE), a foil coil and insulation materials such as epoxy resins and polyimide wire insulation. The dimensions and material properties of the linear actuator configuration are given in Table 1. Furthermore, the voltage distribution in the foil coil is shown in Figure 2.
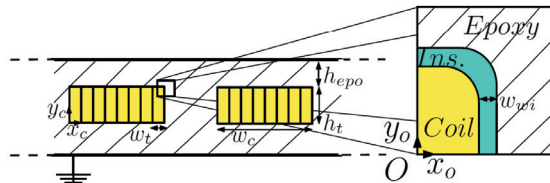

Fig. 1. Section of the linear motor configuration with one foil coil
and without a field control method

Semi-analytical modeling of the linear actuator configuration, as performed in [11], has limited accuracy near corners and edges of conducting regions. Therefore, the linear actuator configuration with the different field control methods field is modeled with 2-D boundary element and finite element method using Integrateds Electro [12]. Electrode profiling, capacitive and refractive field control methods are modeled using the boundary element method. The resistive field control method is modeled using the finite element method since the boundary element method is unable to take nonlinear material properties into account. The simulations are performed in steady state using a frequency of 100 Hz and both the permittivity and the conductivity of the materials are taken into account.

The field control methods are assessed by their capability to mitigate the electric field strength near the edge of the inner turn with origin $O_{xo, yo}$, as shown in Figure. 1. Furthermore, the investigated field control methods are applied such that there is no change in electric loading of the linear actuator. Therefore, the active coil volume and the combined height of the coil and insulating materials remain unchanged for the different field control methods.
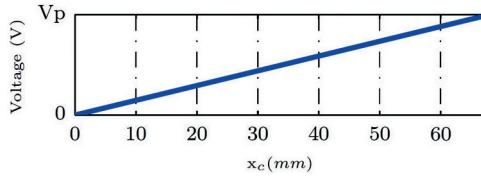
Fig. 2. Potential distribution, with respect to PE,
of the foil coil along half the coil width

3. Electric field control methods

Electric field enhancements are often strongly localized in space, e.g., at electrode edges and corners and, therefore, field control methods are necessary to mitigate electric stress at these locations. These field control methods can be distinguished in two main classes [13]. Firstly, capacitive field control concerns electrode profiling, refractive field control and condenser field control. Secondly, resistive field control concerns semi-conductive layers to control electric stress.

Table 1. Dimensions and material properties of the linear actuator configuration

Variable	Description	Value
r_c	rounding radius of corners	0.01 mm
r_{ep}	radius of electrode profile	2 mm
w_t	turn width	0.3 mm
w_c	0.5 coil width	68 mm
w_{wi}	wire insulation width	0.02 mm
h_{epo}	insulation height epoxy	0.5 mm
h_{seco}	height semi-cond. layer	0.02 mm
W_{cap}	capacitive layer width	0.16 mm
W_{seco}	semi-cond. layer width	0.98 mm
W_{refr}	refractive layer width	0.28 mm
t_{hpl}	thickness high-permittivity layer	0.02 mm
h_t	turn height	4 mm
V_p	peak coil voltage	2500 V
V_{co}	cooling environment voltage	0 V
ε_{epo}	rel. perm., epoxy insulation	3.45
ε_{wi}	rel. perm., wire insulation	3.9
ε_{refr}	rel. perm., refractive layer	10
ε_{cap1}	rel. perm., capacitive layer 1	5
ε_{cap2}	rel. perm., capacitive layer 2	3
ε_{cap3}	rel. perm., capacitive layer 3	2.5
ε_{seco}	rel. perm., semi-cond. layer	3.45
ε_{hpl}	rel. perm., high-permittivity layer	7
σ_{epo}	cond. epoxy insulation	$1\ 10^{-17}$ S/m
σ_{wi}	cond. wire insulation	$3.45\ 10^{-15}$ S/m
σ_{refr}	cond. refractive layer	$3.45\ 10^{-15}$ S/m
σ_{cap}	cond. capacitive layers	$3.45\ 10^{-15}$ S/m
σ_{hpl}	cond. high-permittivity layer	$3.45\ 10^{-15}$ S/m

3.1. Electrode profiling

Electrode profiling mitigates electric field stress by reshaping conducting regions with high-field enhancements. In the linear actuator configuration this is performed by adding a conducting rounded Electrode Profile (EP), as shown in Fig. 3. This electrode profile is electrically connected to the inner or outer turn of the coil and, therefore, no potential difference is present between the electrode profile and the coil. As a result, the charge density, and subsequently the peak electric field strength, is reduced at the corner of the coil.
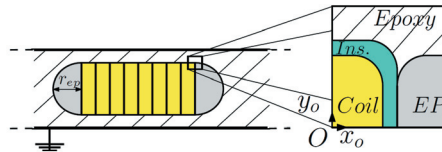

Fig. 3. Section of the linear motor configuration with Electrode Profiling (EP)

3.2. Refractive field control

Refractive field control uses dielectric refraction to mitigate electric field stress. When the electric field strength vector, **E**, meets the interface between two media, with different permittivities, at an angle different than 90 degrees, the direction of the vector will change in the second dielectric. This method is applied in the linear actuator configuration by adding a layer with high permittivity adjacent to the inner and outer turn of the coil, as shown in Figure 4. The relative permittivity of this layer should be several times larger than the surrounding insulation materials for sufficient mitigation of the electric stress [6].
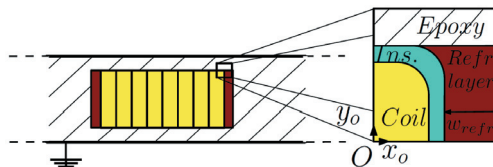

Fig. 4. Section of the linear motor configuration with refractive field control

3.3. Capacitive field control

Capacitive field control consists of multiple dielectric insulation layers with different permittivities which allows the impedance between the coil and the cooling environment to be controlled and, therefore, the electric stress is distributed evenly between the different layers. The required relative permittivity of each insulation layer depends on the relative permittivity and thickness of the wire insulation and the thickness of the insulation layer itself. Typically, materials are required with relative permittivities lower than the wire insulation. The investigated capacitive field control method consists of three layers, with decreasing permittivities between each layer, surrounding the coil and is shown in Figure 5.
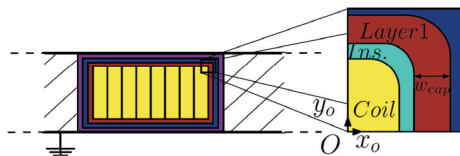
Fig. 5. Section of the linear motor configuration with capacitive field control

3.4. Resistive field control

Resistive field control lowers electric stress by increasing the electrical conductivity in regions with high electric field strengths. In these regions, space charge is formed and creates a counteracting field, which reduces the field enhancement [13]. Typical resistive field grading materials are polymeric composites based on fillers such as silicon carbide, carbon black and zinc-oxide particles. The investigated resistive field control method, as shown in Fig. 6 consists of semi-conductive layers adjacent to the inner and outer turn of the coil. The electric field-dependent conductivity, σ_{sc}, of the semi-conductive layer is given by

$$\sigma_{sc} = 6.17\,10^{-14} - 1.23\,10^{-13}\,E + 1.25\,10^{-19}\,E^2 - 1.22\,10^{-27}\,E^3. \tag{1}$$

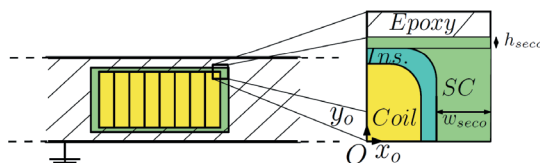where E is the electric field strength.

Fig. 6. Section of the linear motor configuration with resistive field control using
a Semi-Conductive layer (SC)

3.5. Combined field control

The presented combined field control method consist of elements of different field control methods. Firstly, the conducting rounded profile as presented in Section 3.1 is applied. Furthermore, on top of the profile a layer with high permittivity is applied. This layer reduces surface impedance and, therefore, increases the forming of space charge [6]. The investigated combined field control method is shown in Figure 7.
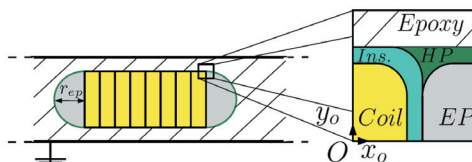

Fig. 7. Section of the linear motor configuration with combined field control, consisting
of an Electrode Profile (EP) and a High-Permittivity layer (HP)

www.czasopisma.pan.pl   PAN   www.journals.pan.pl
POLSKA AKADEMIA NAUK

634   T.A. Van Beek, J.W. Jansen, E.A. Lomonova   Arch. Elect. Eng.

4. Results

The electric field strength of the configuration without a field control method is shown in Figure 8. From this figure it is clear that the peak electric field strength occurs near the corner of the inner turn and is equal to 17.7 kV/mm. Potting materials, such as epoxies, polyurethanes and silicones, typically have a dielectric breakdown strength between 15 and 20 kV/mm. However, these values hold for materials under ideal conditions, without voids, impurities or contaminations. Therefore, the configuration as shown in Figure 1 is likely to fail before it reaches its expected lifetime.

The peak electric field strengths in the linear motor configuration with and without field control methods are summarized in Table 2.
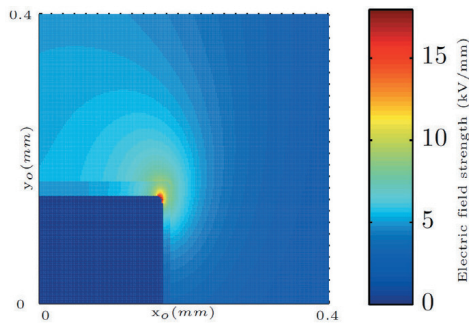

Fig. 8. Electric field distribution of the linear motor configuration without field control method

Table 2: Peak electric field strength in linear motor configuration for the electric field control methods

Field control method	Peak electric field strength (kV/mm)
None	17.7
Electrode profiling	7.1
Refractive	16.1
Capacitive	7.3
Resistive	8.3
Combined	5.8

4.1. Electrode profiling

Applying electrode profiling as field control method results in the electric field distribution as shown in Fig. 9. The peak electric field strength is equal to 7.1 kV/mm. The ability of this field control method to mitigate electric stress is limited by the thickness of the wire insulation. For increasing thickness of the wire insulation the separation between the coil and the electrode profile becomes larger. This results in a redistribution of charge where the charge density at corners increases and, therefore, higher electric field strengths will occur near the corner.

Practical applications with electrode profiling would require combinations of field control methods since an enclosed electrode profile, in combination with a permanent magnet assembly, acts as a damper ring and increase losses.
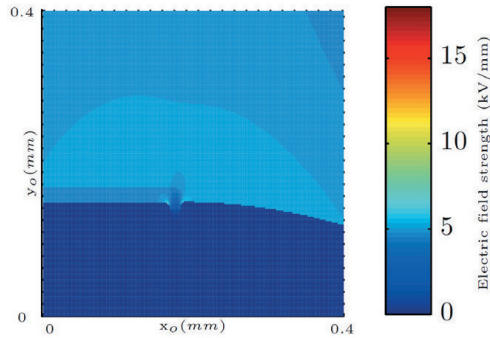
Fig. 9. Electric field distribution of the linear motor configuration with electrode profiling

4.2. Refractive field control

The electric field strength due to the refractive field control method is shown in Figure 10. The peak electric field strength is equal to 16.1 kV/mm. Compared to other field control methods, the attenuation in peak electric field strength is small. This is due to the wire insulation which prevents the refractive layer from directing the electric field vector near the corner of the coil. The, relatively small, achieved level of attenuation is due to forming of space charge in refractive layer and, therefore, lowering the peak electric field strength.
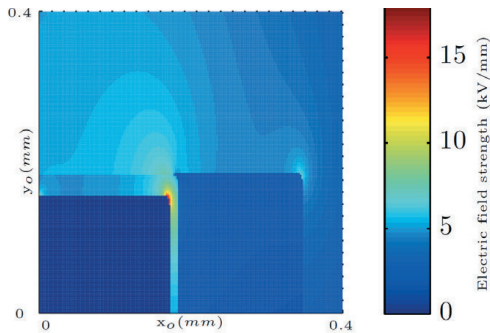

Fig. 10. Electric field distribution of the linear motor configuration with refractive field control

4.3. Capacitive field control

The electric field strength due to capacitive field control is shown in Figure 11. The peak electric field strength is equal to 7.3 kV/mm. The level of mitigation provided by the capacitive field control is limited by the permittivity of the wire insulation since its relative permittivity is typically low (2-4), therefore, the capacitive layers are limited in changing the impedance of each layer and, subsequently, the electric stress in each layer. To distribute the potential evenly, materials with relative permittivities significantly higher and lower than the wire insulation, ε_{wi}, are necessary, while having a high electric breakdown strength as well. However, obtaining materials with the proper material characteristics might be difficult, since they are not widely available [6]. Furthermore, all capacitive layers should be void-free since

voids in regions with high relative permittivity are prone to high levels of electric stress [14] and initiate partial discharge.
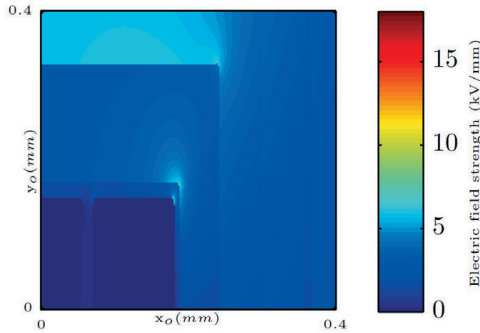

Fig. 11. Electric field distribution of the linear motor configuration with capacitive field control

4.4. Resistive field control

The peak electric field strength due to the resistive field control method is equal to 8.3 kV/mm. The limitation of this field control method is mainly determined by the nonlinearity of the semi-conductive layer where nonlinearity is defined as the ratio in conductivity between the resistive and conductive regime of the material. Semi-conductive materials with higher non-linearity reduces the peak electric field strength. However, materials with higher nonlinear-ity increase ohmic losses in the semi-conductive layer and are more difficult to develop and manufacture [13].
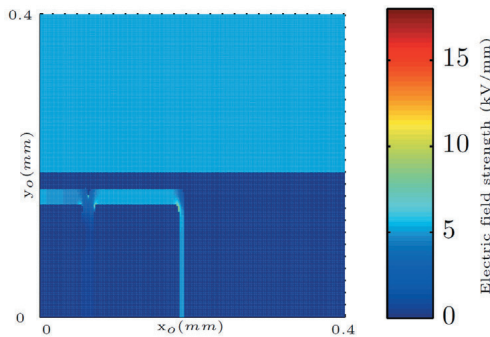

Fig. 12. Electric field distribution of the linear motor configuration with resistive field control

4.5. Combined field control

The electric field distribution of the combined field control method is shown in Figure 13. The peak electric field strength due to the combined field control method is equal to 5.8 kV/mm. As with electrode profiling, the effectiveness of this method is limited by the thickness of the wire insulation. Furthermore, voids in the layer with high permittivity should be avoided as explained in Section 4.3.
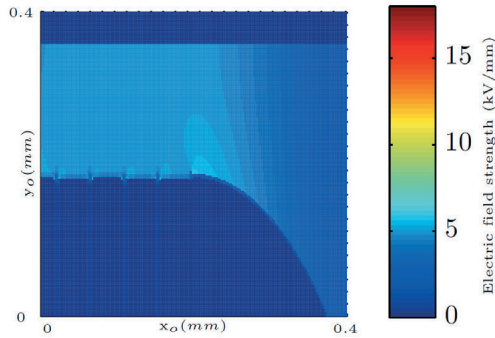
Fig. 13. Electric field distribution of the linear motor configuration
with combined field control

5. Sensitivity to misalignment

Manufacturing tolerances and positioning errors of, for instance, field control methods can cause misalignment between the foil coil and the field control method. Due to the misalignment, protrusions and edges are introduced which result in higher electric field strengths and, therefore, lower effectiveness of the field control methods.

The sensitivity of electrode profiling, resistive and the combined field control method to misalignment errors is investigated by varying the height of the resistive layer $h^*_{\sec o}$, in the case of the resistive field control method, and the radius of the electrode profile r^*_{ep}, in the cases of electrode profiling and the combined field control method. Misalignment, in the case of the capacitive field control method, is investigated by varying the thickness of the first layer, w^*_{cap1}, thereby either increasing or decreasing the thickness of the second layer. The relation between the misalignment error and the investigated geometry variables is given by

$$h^*_{\sec o} = h_{\sec o} + \varphi, \tag{2}$$

$$r^*_{ep} = r_{ep} + \varphi, \tag{3}$$

$$w^*_{cap1} = w_{cap} + \varphi, \tag{4}$$

where φ is the misalignment error, ranging from –0.1 to 0.1 mm.

Furthermore, only positive misalignment is considered for the resistive field control method and the refractive method is omitted in the sensitivity investigation due to its low effectiveness as shown in Section 4.2.

In Figure 15 the peak electric field strength is shown for electrode profiling, resistive, capacitive and the combined field control method for different misalignment errors.
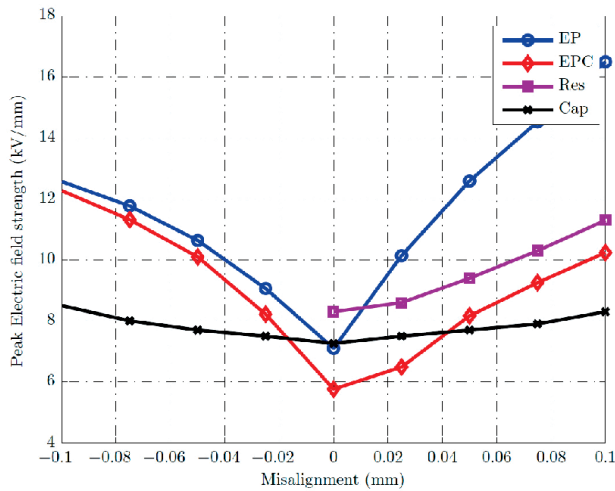
Fig. 15. Peak electric field strength for electrode profiling (EP), resistive (Res), capacitive (Cap) and the combined field control method (EPC) for different amplitudes of misalignment

From Figure 15 it is clear that any misalignment error negatively affect the effectiveness of the field control methods. The sensitivity of electrode profiling, resistive and combined field control methods to misalignment errors is caused by the relative low insulation height, h_{epo}. Therefore, positive misalignment errors decrease the insulation thickness significantly and, subsequently, increases peak electric field strength.

With the exception of the capacitive field control method, the resistive field control method is the least sensitive field control method. The peak electric field strength increases from 8.3 to 11.3 kV/mm for a misalignment of 0.1 mm whereas electrode profiling and the combined field control method increase with 9.4 and 4.5 kV/mm to 16.5 and 10.2 kV/mm, respectively.

For negative alignment errors electrode profiling and the combined field control method show identical behaviour. Negative alignment results in an increased distance between the field control method and the corner of the coil. Therefore, the surface charge density at the corner of the coil increases and, subsequently, the peak electric field strength increases.

As shown in Figure 15 the capacitive field control method has peak electric field strengths of 7.3 and 8.5 kV/mm for a misalignment of 0 and 0.1 mm, respectively. Compared to the other field control methods, the capacitive field control method is relatively insensitive to misalignment errors, i.e. variation in width of the capacitive layers. In the capacitive field control method misalignment causes a change in the capacitance of the respective layers and, therefore, a different voltage distribution between the capacitive layers. However, this misalignment has not a significant influence on the electric field distribution. For instance, increased layer width due to misalignment results in a lower capacitance for this layer and, therefore, a higher potential drop. Although the potential drop across this layer is increased, also the width of the respective layer is increased. Therefore, misalignment has a limited effect on the amplitude of the electric field strength in the respective layer.

6. Conclusions

In this paper, multiple electric field control methods have been investigated on their capability to mitigate electric field stress for foil coils in high-voltage coreless linear actuators and the sensitivity of field control methods to misalignment. The methods comprise resistive, refractive, capacitive, electrode profiling and a combined approach as field control solutions which aim at reducing the peak electric field strength in areas with high-field enhancements, such as near an edge of a foil coil. The electrode profiling, refractive, capacitive and combined field control methods are modeled using a 2-D boundary element method, whereas the resistive field control method is modeled using a 2-D finite element method. Most of the presented field control methods reduce the peak electric field strength near the corner of the foil coil significantly, except for the refractive method. The refractive method reduces the peak electric stress only by 10%, whereas electrode profiling, capacitive, resistive and combined field control method reduce the peak field strength by 60, 59, 53, 67%, respectively.

Furthermore, the sensitivity of the field control methods to misalignment has been investigated by altering the geometry of the field control methods. For either positive or negative misalignment, the effectiveness of the field control methods is reduced. For the capacitive field control method the peak electric field strength increase from 7.3 to 8.3 kV/mm for a misalignment of 0.1 mm whereas similar misalignment for electrode profiling results in an increase in peak electric field strength from 7.1 to 16.5 kV/mm. Furthermore, the combined and resistive field control method have an increase of peak electric field strength of respectively 4.5 and 3.0 kV/mm for a misalignment of 0.1 mm.

References

[1] Wang P., Cavallini A., and Montanari G., *The influence of impulsive voltage frequency on pd features in turn insulation of inverterfed motors*. Electrical Insulation and Dielectric Phenomena (CEIDP), 2014 IEEE Conference on, pp. 35-38 (2014).

[2] Strobl R., Haverkamp W., Malin G., Fitzgerald F., *Evolution of stress control systems in medium voltage cable accessories*. in Transmission and Distribution Conference and Exposition, IEEE/PES 2: 843-848 (2001).

[3] Donzel L., Greuter F., Christen T., *Nonlinear resistive electric field grading part 2: Materials and applications*. Electrical Insulation Magazine, IEEE 27: 18-29 (2011).

[4] Li J., et. al. *Electric field calculation and grading ring optimization of composite insulator for 500 kv ac transmission lines*. in Solid Dielectrics (ICSD), 2010 10th IEEE International Conference on, pp. 1-4 (2010).

[5] N. Hayashi, et.al. *Electric field control by permittivity functionally graded materials and their lightning impulse withstand voltages for surface breakdown*. in Electrical Insulation, Conference Record of the 2002 IEEE International Symposium on, pp. 260-263 (2002).

[6] Roberts A., *Stress grading for high voltage motor and generator coils*. Electrical Insulation Magazine, IEEE 11: 26-31, (1995).

[7] Burns N., Eichhorn R., Reid C., *Stress controlling semiconductive shields in medium voltage power distribution cables*. Electrical Insulation Magazine, IEEE 8: 824, Sept. (1992).

[8] E. Sharifi, et.al. *Iec qualification test applied to capacitively graded 13.8 kv bar samples energized with repetitive fast pulses*. in Electrical Insulation Conference (EIC), 2011, pp. 402-406 (2011).

[9] El-kishky H., *Experience with development and evaluation of corona-suppression systems for hv rotating machines*. Dielectrics and Electrical Insulation, IEEE Transactions on 9: 569-576 (2002).

www.czasopisma.pan.pl   PAN   www.journals.pan.pl

POLSKA AKADEMIA NAUK

640   *T.A. Van Beek, J.W. Jansen, E.A. Lomonova*   Arch. Elect. Eng.

[10] van Beek T., Jansen J., Lomonova E., *Electric Field Control Methods for Foil Coil in High-Voltage Linear Actuators*", Proceedings of the 10th International Symposium on Linear Drives for Industry Applications (LDIA 2015).

[11] T. van Beek, et.al. *Electrostatic modeling of cavities inside linear actuators*. Journal of Physics: Conference Series, Volume 646, 2015..

[12] Electro V9.3 Quick Start Guide. Winnipeg, Canada: Integrated Engineering Software (2015).

[13] Christen T., Donzel L., and Greuter F., *Nonlinear resistive electric field grading part 1: Theory and simulation*. Electrical Insulation Magazine, IEEE 26: 47-59, (2010).

[14] Knuffel E., Zaengl W., Knuffel J., *High Voltage Engineering Fundamentals*, Butterworth-Heinemann (2000).